Disturbed Epidermal Structure in Mice with Temporally Controlled Fatp4 Deficiency

Thomas Herrmann,* Hermann-Josef Gröne,† Lutz Langbein,‡ Iris Kaiser,* Isabella Gosch,* Ute Bennemann,* Daniel Metzger,§¶ Pierre Chambon,§¶ Adrian Francis Stewart,# and Wolfgang Stremmel*

*Department of Internal Medicine IV, University of Heidelberg, Heidelberg, Germany; Departments of †Cellular and Molecular Pathology and ‡Cell Biology, German Cancer Research Center, Heidelberg, Germany; §Institut de Génétique et de Biologie Moléculaire et Cellulaire, CNRS/INSERM/ULP, Illkirch Cedex, France; ¶Institut Clinique de la Souris, Illkirch Cedex, France; #Genomics, BioInnovationsZentrum, The University of Technology Dresden, Dresden, Germany

So far, little is known about the physiological role of fatty acid transport protein 4 (Fatp4, Slc27a4). Mice with a targeted disruption of the *Fatp4* gene display features of a human neonatally lethal restrictive dermopathy with a hyperproliferative hyperkeratosis, a disturbed epidermal barrier, a flat dermal–epidermal junction, a reduced number of pilo-sebaceous structures, and a compact dermis, demonstrating that Fatp4 is necessary for the formation of the epidermal barrier. Because Fatp4 is widely expressed, it is unclear whether intrinsic Fatp4 deficiency in the epidermis alone can cause changes in the epidermal structure or whether the abnormalities observed are secondary to the loss of Fatp4 in other organs. To evaluate the functional role of Fatp4 in the skin, we generated a mouse line with Fatp4 deficiency inducible in the epidermis. Mice with epidermal keratinocyte-specific Fatp4 deficiency developed a hyperproliferative hyperkeratosis with a disturbed epidermal barrier. These changes resemble the histological abnormalities in the epidermis of newborn mice with total Fatp4 deficiency. We conclude that Fatp4 in epidermal keratinocytes is essential for the maintenance of a normal epidermal structure.

Key words: conditional mutagenesis/differentiation/epidermis/skin barrier/Slc27a4
J Invest Dermatol 125:1228–1235, 2005

Recently, we generated mice with a targeted disruption of the *Fatp4* gene within intron 2 to analyze the functional significance of Fatp4 (Herrmann *et al*, 2003). The *Fatp4* null mice displayed features of a human neonatally lethal restrictive dermopathy (Holbrook *et al*, 1987; Dean *et al*, 1993). Their skin was characterized by a hyperproliferative hyperkeratosis with a disturbed epidermal barrier, a flat dermal–epidermal junction, a reduced number of pilo-sebaceous structures, and a compact dermis. The rigid skin consistency resulted in an altered body shape with facial dysmorphia, generalized joint flexion contractures, and impaired movement, including suckling and breathing deficiencies. The morphological alterations were accompanied by a severely compromised epidermal barrier function. Lipid analysis demonstrated a disturbed fatty acid composition of epidermal ceramides with a reduced proportion of very long chain fatty acid residues within the ceramide fraction of Fatp4-deficient epidermis. These findings revealed a previously unknown, essential function of Fatp4 in the formation of the epidermal barrier. Another mouse line carrying a naturally occurring mutation in exon 3 of the *Fatp4* gene leading to Fatp4 deficiency (Moulson *et al*, 2003) displayed the same phenotype, confirming our findings. But another genetically engineered mouse line with a targeted disruption of the *Fatp4* gene (Gimeno *et al*, 2003) where exons 2 and 3 were replaced by a selectable marker cassette exhibited a far more severe phenotype with early embryonic lethality before day 9.5 of gestation. The reason for the differences between the two mouse lines with disruption of the *Fatp4* gene within intron 2 and exon 3, respectively, and the mouse line with disruption of the *Fatp4* gene at the 5′ side of exon 2 is unclear.

Immunofluorescence microscopy localized Fatp4 to the *stratum granulosum* and the *stratum spinosum* of the epidermis (Herrmann *et al*, 2003). But it remained unclear whether the lack of Fatp4 in the epidermis was the primary cause of the dominant skin phenotype of mice with generalized Fatp4 deficiency or whether the alterations in the skin architecture were secondary phenomena because of the lack of Fatp4 elsewhere. To answer this question, we used a variation of Cre/lox conditional mutagenesis based on ligand inducible recombination (Logie and Stewart, 1995; Metzger *et al*, 1995). In addition to placing loxP sites strategically within the *Fatp4* gene, a Cre recombinase—mutant estrogen receptor fusion protein (ER^{T2}) was used to render conditional mutagenesis of *Fatp4* dependent upon the administration of tamoxifen (Feil *et al*, 1997; Brocard *et al*, 1998; Metzger and Chambon, 2001). Because Cre-ER^{T2} expression was directed by the K14 promoter (Li *et al*, 2000), conditional mutagenesis of *Fatp4* was confined to epidermal keratinocytes after tamoxifen administration. Thereby, we show that Fatp4 in the epidermis itself is essential for the maintenance of a normal epidermal structure.

Abbreviations: AFT, after the first tamoxifen treatment; X-gal, 5-bromo-4-chloro-3-indolyl-β, D-galactopyranoside

Results

Generation of *Fatp4* mutant mice The strategy used for the generation of *Fatp4* mutant mice with epidermis-specific *Fatp4* inactivation is shown in Fig 1*A*. To generate mice with a floxed *Fatp4* allele ($Fatp4^{flox/wt}$), $Fatp4^{neoflox/wt}$ mice were crossed with transgenic mice expressing FLPe recombinase (Rodriguez *et al*, 2000). $Fatp4^{flox/wt}$ mice were crossed with *K14-Cre-ER*^{T2} transgenic mice (Li *et al*, 2000) to generate $Fatp4^{flox/wt}$ *K14-Cre-ER*$^{T2(tg/0)}$ double-mutant mice carrying a floxed *Fatp4* allele and the *K14-Cre-ER*^{T2} transgene. To generate mice with an *Fatp4* null allele ($Fatp4^{neo\Delta ex3/wt}$), $Fatp4^{neoflox/wt}$ mice were crossed with *PGK-Cre* transgenic mice (Schwenk *et al*, 1995). $Fatp4^{flox/wt}$ *K14-Cre-ER*$^{T2(tg/0)}$ mice were crossed with $Fatp4^{neo\Delta ex3/wt}$ *K14-Cre-ER*$^{T2(0/0)}$ mice to generate $Fatp4^{neo\Delta ex3/flox}$ *K14-Cre-ER*$^{T2(tg/0)}$ mice, which were injected with tamoxifen to generate mice with epidermis-specific inactivation of *Fatp4*, now termed *esi-Fatp4*.

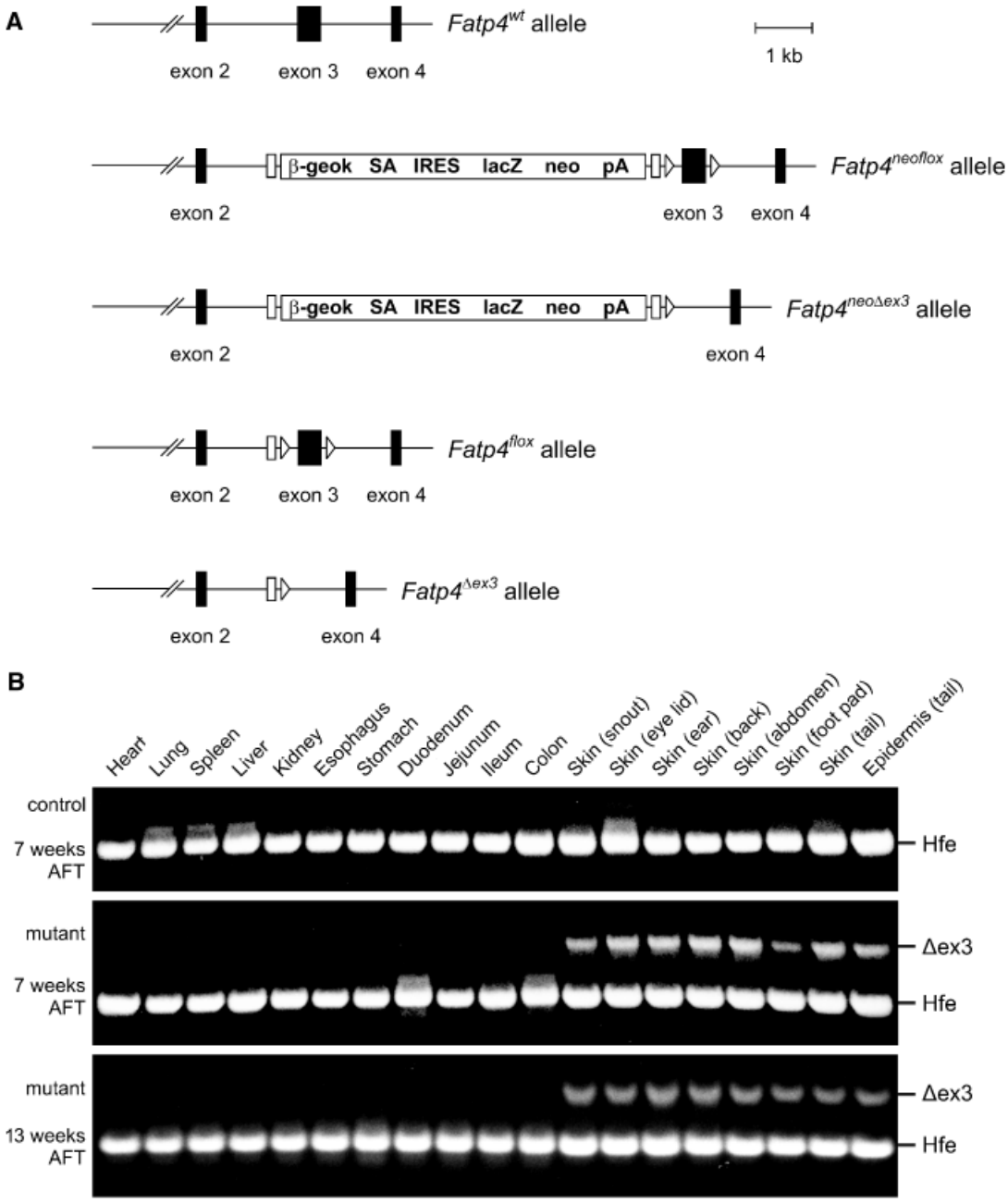

Figure 1
Tamoxifen-induced *Fatp4* null mutation in adult mouse epidermis mediated by *K14-Cre-ER*^{T2}. (*A*) *Fatp4* locus before ($Fatp4^{wt}$) and after ($Fatp4^{neoflox}$) homologous recombination with the targeting vector insert. LoxP sites are depicted as open triangles, and FRT sites as open rectangles. FLPe recombinase converts the allele $Fatp4^{neoflox}$ into the allele $Fatp4^{flox}$, which lacks the neomycin resistance cassette. Cre recombinase converts the allele $Fatp4^{flox}$ into the null allele $Fatp4^{\Delta ex3}$, which lacks exon 3, and the allele $Fatp4^{neoflox}$ into the null allele $Fatp4^{neo\Delta ex3}$, which lacks exon 3 but still contains the neomycin resistance cassette. (*B*) PCR genotype analysis of DNA from various tissues 7 and 13 wk after the first tamoxifen treatment (AFT). An ethidium bromide-stained agarose gel containing amplification products from *K14-Cre-ER*$^{T2(0/0)}$ $Fatp4^{neo\Delta ex3/flox}$ (control) and *K14-Cre-ER*$^{T2(tg/0)}$ $Fatp4^{neo\Delta ex3/flox}$ (mutant, *esi-Fatp4*) mice, respectively, is shown. A PCR with *Hfe*-specific primers served as the control reaction.

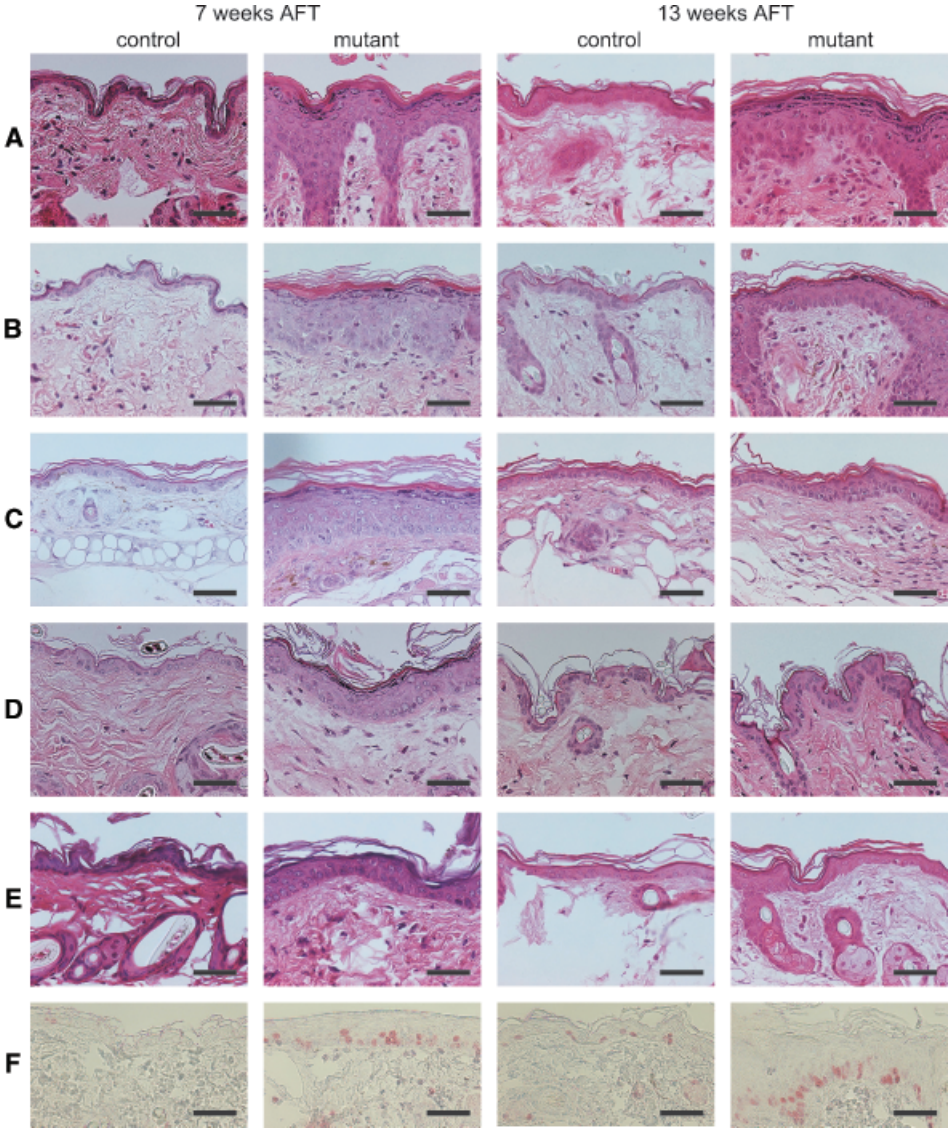

Figure 2
Abnormalities generated in skin of adult mouse by tamoxifen-induced disruption of *Fatp4* mediated by *K14-Cre-ER^{T2}*. Skin of mutant mice and control littermates 7 and 13 wk after the first tamoxifen treatment (AFT). Skin from the snout (*A*), eyelid (*B*), ear (*C*), back (*D*), and foot pad (*E*) was stained with hematoxylin and eosin. In comparison with control epidermis, *Fatp4* mutant (*esi-Fatp4*) epidermis exhibited more cell layers in the *stratum spinosum* and the basal layer. (*F*) Immunohistochemical analysis using anti-Ki-67 antibodies showed an increase in the number of positive cells in the basal layer and also several positive suprabasal cells in the skin from the eyelid of *esi-Fatp4* mice compared with control mice. *Scale bar*, 50 μm.

PCR analysis was used to identify the different genotypes and to detect the Cre-mediated recombination of the allele *Fatp4^{flox}* to the allele *Fatp4$^{\Delta ex3}$* (Fig 1*B*).

Phenotype of *Fatp4* mutant mice Mice with epidermis-specific *Fatp4* deficiency (*esi-Fatp4* mice) did not show any gross abnormality in comparison with control littermates neither 7 nor 13 wk after the first tamoxifen treatment (AFT). Their behavior and gross appearance were also normal. Only histological examination revealed distinct changes.

The stratum corneum of *esi-Fatp4* mice was considerably thicker than that of control littermates (Fig 2). The *stra-*

Figure 3
Differentiation of foot sole skin of *Fatp4* mutant and control mice, as shown by immunofluorescence microscopy. To the right of each of the immunofluorescence micrographs are the respective phase-contrast images of the same sections. (*A*) Immunostaining of Fatp4 in mouse foot sole skin. Fatp4 is detectable only at the cell margins of the *stratum granulosum* subadjacent to the *stratum corneum* (sc) of control mice (*white open arrow*). In *Fatp4* mutant mice, no specific labelling can be observed (*yellow open arrow*). (*B*) Immunostaining of keratin K14 in plantar epidermis. Whereas K14 is restricted to the *stratum basale* (sb) of control mice, it is also detected in the lower/middle cells of the *stratum spinosum* (ss) of *Fatp4* mutant mice (*yellow open arrow*). (*C*) Immunostaining of K6 is seen in basal and some lower suprabasal cells in control mice (*white open arrow*), as normally observed in foot sole epidermis. In the *Fatp4* mutant mice, this staining includes all living layers of the foot sole (*yellow bracket*). (*D*) The staining pattern using antisera against K10 shows all suprabasal cells (*stratum spinosum* and *stratum granulosum*; *white bracket*, ss + sg) to be positive, with considerable widening of both layers in *Fatp4* mutant mice (*yellow bracket*, ss + sg). (*E*) Keratin K2e is expressed very late during terminal keratinocyte differentiation of the skin and is detectable only in the *stratum granulosum* cells of control mice (*white bracket*, sg), whereas in *Fatp4* mutant mice it is strongly increased in both the *stratum spinosum* and *stratum granulosum* (*yellow bracket*, ss + sg). Loricrin (*F*), filaggrin (*G*), and transglutaminase 1 (*H*) are typical proteins of the cornified envelope and specific components of the process of terminal keratinocyte differentiation. They all can be detected in the upper stratum spinosum and in the *stratum granulosum* of control mice (*F–H*, *white brackets*). In *Fatp4* mutant mice, these proteins are regularly seen in the uppermost *stratum spinosum* as well as most prominently in the broadened *stratum granulosum* (*F–H*, *yellow brackets*). (*I*) The presence of claudin-1 in the cell–cell borders of all layers of the skin (*white bracket*, ss-sg) indicates an intact tight junction barrier in both kinds of mice, whereas in *Fatp4* mutant mice the staining is restricted to the *strata spinosum* and *granulosum* (*yellow bracket*, ss + sg). Blue staining: DAPI-stained nuclei. gl, sebaceous gland. *Scale bar*, 50 μm.

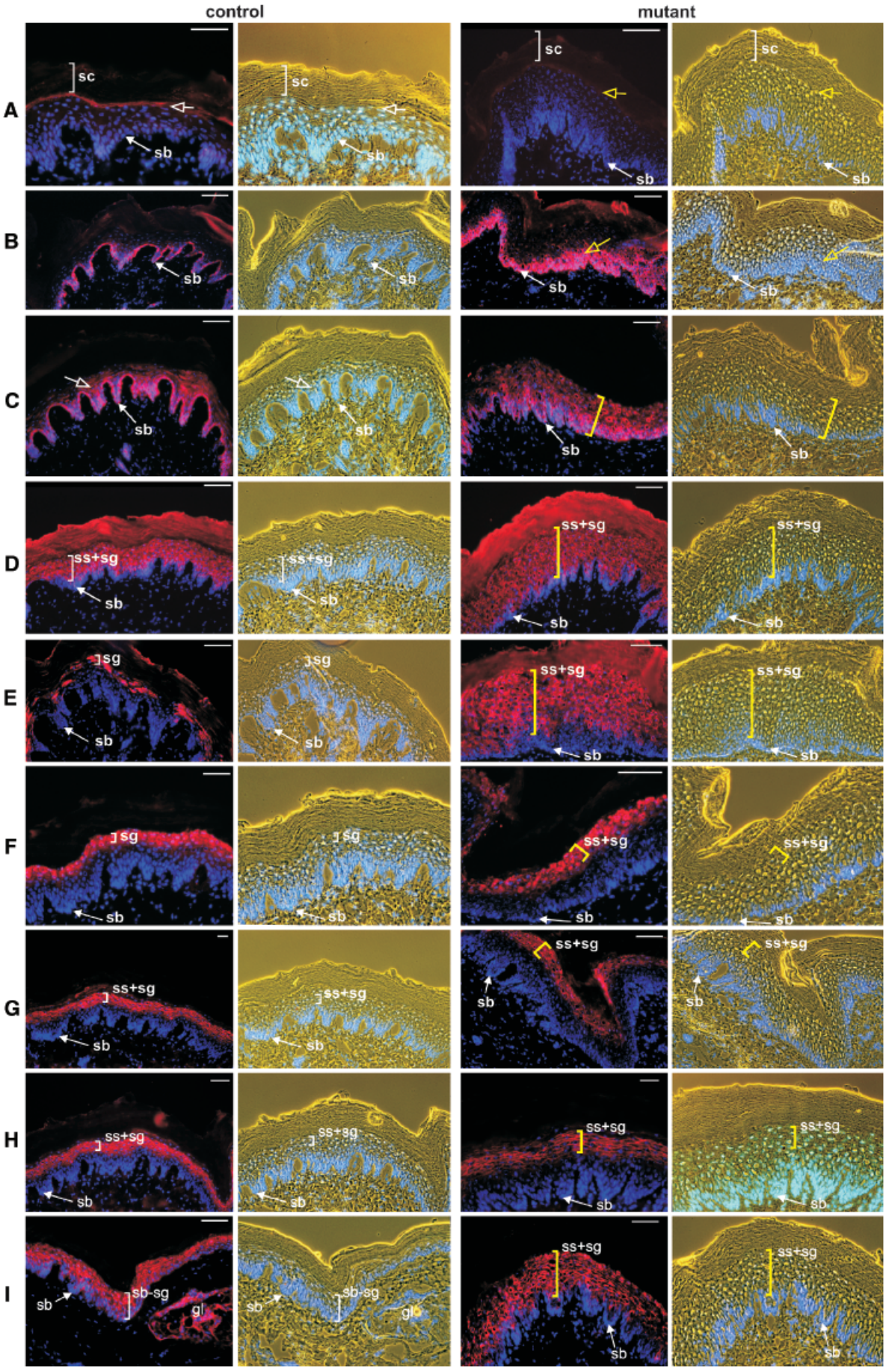
control
mutant
A
B
C
D
E
F
G
H
I
sc
sb
sg
ss+sg
sb-sg
gl

tum spinosum was characterized by an increased number of cell layers. In comparison with newborn mice with generalized Fatp4 deficiency, however, the alterations were less pronounced. The flat dermal–epidermal junction, the reduced number of pilo-sebaceous structures, and the condensed dermis with compact collagen fibers present in newborn mice with generalized Fatp4 deficiency could not be observed in adult *esi-Fatp4* mice, neither 7 nor 13 wk AFT. In addition, no ultrastructural differences between control and transgenic mice could be detected, including lamellar membranes as well as the number and shape of lamellar bodies (data not shown).

All other organs, including the brain, intestine, liver, spleen, kidneys, myocardium, lung, thymus, and skeletal muscle (not shown), examined by light microscopy appeared normal in *esi-Fatp4* mice both 7 and 13 wk AFT.

Immunohistochemical analysis revealed an increased number of Ki-67-positive nuclei in the basal layer of *esi-Fatp4* mouse epidermis in comparison with control mouse epidermis (7 wk AFT: 45% *vs* 9%; 13 wk AFT: 42% *vs* 19%). Whereas in control mouse skin all positive nuclei were located in the basal layer of the epidermis or in the outer root sheath or matrix of hair follicles (data not shown), in *esi-Fatp4* mouse skin some Ki-67-positive cells were observed in the first suprabasal layer (Fig 2*F*). Thus, the observed hyperkeratosis could be classified as a hyperproliferative hyperkeratosis.

The immunofluorescence studies were performed on foot sole and on snout epidermis (data not shown). For Fatp4 immunofluorescence microscopy, we used an antiserum that we generated against a specific peptide (Herrmann *et al*, 2003). By using staining protocols without detergent addition in any of the fixation and incubation steps (see Materials and Methods), a decoration along the cell margins of the *stratum granulosum* was seen in $Fatp4^{neo\Delta ex3/flox}$ $K14\text{-}Cre\text{-}ER^{T2(0/0)}$ mice (henceforth termed control mice; Fig 3*A*, *white open arrow*), and a very faint but nonspecific cytoplasmic staining (cf. Herrmann *et al*, 2003) was seen in the keratinocytes of the lower *stratum basale*. This specific Fatp4 staining was not detectable in tamoxifen-treated $Fatp4^{neo\Delta ex3/flox}$ $K14\text{-}Cre\text{-}ER^{T2(tg/0)}$ mice (*esi-Fatp4* mice; Fig 3*A*, *yellow open arrow*). Special aspects could be observed when investigating skin appendages. Besides the interfollicular epidermis, in control snout skin, Fatp4 was most prominent at the cellular margins of trichocytes of hair follicle cortex and keratinocytes of the inner root sheath and less pronounced in those of the outer root sheath (Fig 4*A*, *B*). Furthermore, the epithelial cells of the sebaceous glands were also positive for Fatp4 (Fig 4*C*). In mutant animals, as already mentioned, Fatp4 staining of the interfollicular epidermis was no longer detectable and the staining in the sebaceous glands and the outer root sheath was also lost (Fig 4*D*). Remarkably, the staining of the hair follicle cortex, the inner root sheath, and the companion layer was not affected (Fig 4*D*, *inset* and *E*). No specific Fatp4 staining of dermal components could be detected.

As keratin K14 is expressed neither in the hair fiber nor in the inner root sheath (Langbein *et al*, 1999, 2001, 2002b, 2003; for a review see Langbein and Schweizer, 2005), the maintenance of Fatp4 staining after the tamoxifen-induced, K14 promoter-controlled inactivation of *Fatp4* in these K14-negative tissue compartments is reasonable. Otherwise, in the K14-positive sebaceous glands (Hughes *et al*, 1996) and the outer root sheath (Coulombe *et al*, 1989), Fatp4 staining was, like in the interfollicular epidermis, lost. These results can clearly be assessed as an "internal proof" of the specificity and efficiency of the knockout technique used in this work.

The skin of *esi-Fatp4* mice was hyperplastic, hyperkeratotic, and parakeratotic. Therefore, we investigated the differentiation of keratinocytes, particularly the occurrence and distribution of specific keratins and other proteins of the cornified envelope, by using standard protocols including detergent permeabilization (see Materials and Methods). Keratin K14 (Fig 3*B*) was markedly restricted to the *stratum basale* of control skin. The skin of *esi-Fatp4* mice showed a comparable immunostaining pattern but with K14 labelling extended to the first or more suprabasal layers (Fig 3*B*, *yellow open arrow*), indicative of increased cell proliferation in the *Fatp4* mutant skin. This proliferative characteristic of the *esi-Fatp4* epidermis was also demonstrable by the intense reaction for keratin K6 (Fig 3*C*): whereas in the foot sole epidermis of control mice typically only the keratinocytes of the basal layer and few suprabasal cells within the secondary ridges were positive for K6 (Fig 3*C*, *white bracket*), in *esi-Fatp4* mouse cells, this keratin was labelled in the basal and also in the suprabasal layers, in the *stratum spinosum*, and particularly in the *stratum granulosum* (Fig 3*C*, *yellow bracket*). Strong keratin K10 reactivity was observed in all living suprabasal cell layers (Fig 3*D*, *white bracket*, ss + sg), but appeared much broader in the hyperkeratotic foot sole of *esi-Fatp4* mice (Fig 3*D*, *yellow bracket*, ss + sg). Neither the *stratum basale* nor the *stratum corneum* reacted in either kind of mice. The immunostaining of keratin K2e was restricted to the keratinocytes of the *stratum granulosum* in control mice (Fig 3*E*; *white bracket*, sg), whereas it was greatly widened, extending to the cells of the upper *stratum spinosum*, in *esi-Fatp4* mice (Fig 3*E*; *yellow bracket*, ss + sg). The stage of cornification of the skin keratinocytes was investigated by the immunolocalization of loricrin (Fig 3*F*), filaggrin (Fig 3*G*), and transglutaminase I (Fig 3*H*): all of these proteins were seen in their typical localizations in both *esi-Fatp4* and control animals, the only consistent difference being that more cell layers showed immunoreactivity in the skin of *esi-Fatp4* mice, indicative of the hyperkeratinization (Fig 3*F–G*, *yellow brackets*).

Immunohistochemical staining of the tight junction proteins claudin-1, occludin, and protein ZO-1 virtually reproduced their typical wild-type localization (cf. Morita *et al*, 1999; Brandner *et al*, 2002; Langbein *et al*, 2002a) i.e. occludin exclusively in the *stratum granulosum* (data not shown), whereas protein ZO-1 (data not shown) and claudin-1 could also be detected at the cell margins of cells of the lower strata (Fig 3*I*, *white bracket*, sb-sg; cf. also Morita *et al*, 1999; Brandner *et al*, 2002; Langbein *et al*, 2002a). In the *Fatp4* mutant animals, both proteins were often detected in the additional layers of the thickened skin. Remarkably, under these conditions, claudin-1 was no longer detectable in the *stratum basale* of *esi-Fatp4* mice (Fig 3*I*, *yellow bracket*, ss + sg).

Epidermal barrier function in *esi-Fatp4* mice To examine whether the observed abnormal skin structure might also be associated with an impaired skin barrier function, two different techniques were applied. The substrate 5-bromo-4-chloro-3-indolyl-β, D-galactopyranoside (X-gal) penetrated *esi-Fatp4* skin, where it was cleaved to produce a colored precipitate by endogenous β-galactosidase activity, whereas the skin of control mice was impermeable (Fig 4*F*). In another set of experiments it was shown that the fluorescent dye Lucifer yellow permeated throughout the entire epidermis in *esi-Fatp4* mice; in contrast, it did not pass through the upper layers of the *stratum corneum* in control mice (Fig 4*G*). Thus, we concluded that the abnormal epidermal structure of *esi-Fatp4* mice was accompanied by a compromised epidermal barrier function.

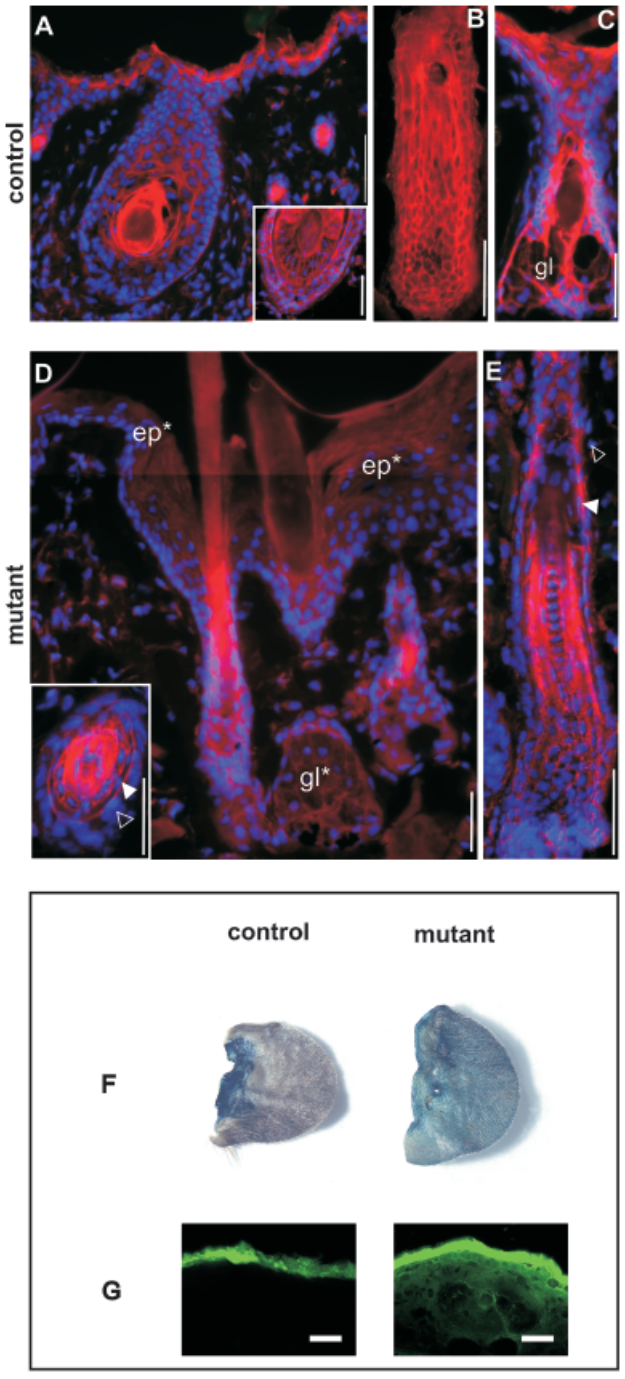

Discussion

Mice with generalized Fatp4 deficiency exhibit a characteristic phenotype with distinct abnormalities in the structure and a disturbed barrier function of the epidermis (Herrmann *et al*, 2003; Moulson *et al*, 2003). How Fatp4 deficiency leads to these severe alterations is still unclear. As Fatp4 acts as an acyl-CoA synthetase for long and very long chain fatty acids (Herrmann *et al*, 2001; Hall *et al*, 2005) and *Fatp4*−/− mice exhibit a disturbed fatty acid composition of epidermal ceramides (Herrmann *et al*, 2003), Fatp4 might play an important role in the epidermal ceramide metabolism.

The mutation within the *Fatp4* gene of our mouse line and the Fatp4-deficient mouse line described by Moulson *et al* (2003) is located within intron 2 and exon 3, respectively. Because we generated a gene trap vector to target the *Fatp4* gene with a mutant multipurpose *Fatp4* allele, we had to integrate the cassette with the selectable marker after the first coding exon, i.e., after exon 2. Another mouse line with a disruption of the *Fatp4* gene at the 5′ side of exon 2 exhibits a far more severe phenotype with early embryonic lethality before gestational day 9.5 (Gimeno *et al*, 2003). The reason for this difference is still elusive. It has been speculated that the disruption of intron 2 or exon 3, respectively, might give rise to a trunkated form of Fatp4 with a rest activity leading to a less severe phenotype than observed when the *Fatp4* gene is disrupted within exon 1. This truncated protein, however, would carry only the first 53 amino acids of Fatp4, whereas the length of the total deduced Fatp4 amino acid sequence is 643 amino acids.

Fatp4 is widely expressed in many organs. Its physiological function in these organs has so far remained elusive. The gene is also strongly expressed in the skin, as we have shown at the RNA level by Northern blot analysis (Herrmann *et al*, 2001) and quantitative RT-PCR (not shown), as well as at the protein level by immunofluorescence (Herrmann *et al*, 2003). But proof has not been provided that the lack of Fatp4 in the epidermis causes the phenotype of Fatp4-deficient mice. It might be conceivable that the lack of Fatp4 in another tissue or other tissues causes secondary effects on the generation and maintenance of the epidermal structure. To find out whether Fatp4 indeed plays a pivotal role in the

Figure 4
Appendages in snout skin of *Fatp4* mutant and control mice, as shown by immunofluorescence microscopy, and disturbed epidermal barrier in *esi-Fatp4* mice. (*A–C*) In control mice, Fatp4 – besides the interfollicular epidermis – can clearly be detected in skin appendages, in the hair follicle, in particular, in the outer root sheath and most prominently in the inner root sheath and in the hair cortex (cross-section, *inset* in (*A*); longitudinal section in (*B*)). Note the positive large whisker and small pelage follicles (*A*). The sebaceous glands are also clearly positive for Fatp4 (*C*). (*D–E*) In mutant mice (7 wk AFT), Fatp4 staining is missed in the interfollicular skin (*D*, ep*), the sebaceous glands (*D*, gl*), and the hair follicle outer root sheath (*open triangles* in the *inset* in (*D*, *E*)). Note that the inner root sheath and the hair cortex remain positive for Fatp4 in *esi-Fatp4* mice. Remarkably, the hair follicle companion layer also remains Fatp4 positive (*triangle* in *E*). (*F*) Access of 5-bromo-4-chloro-3-indolyl-β, D-galactopyranoside (X-gal) to ear skin. Control epidermis is impermeable to X-gal. In contrast, X-gal permeates *Fatp4* mutant skin, where it is cleaved by endogenous β-galactosidase activity to produce a colored precipitate. (*G*) Diffusion of Lucifer yellow in ear skin. The fluorescent dye Lucifer yellow does not pass the upper layers of the *stratum corneum* in control mice. In contrast, in *Fatp4* mutant mice it permeates the entire epidermis. *Scale bar*, 50 μm (*A–E*, *G*).

epidermis for the maintenance of a normal skin structure, the generation of a mouse line with keratinocyte-specific Fatp4 deficiency (Li *et al*, 2000; Metzger and Chambon, 2001) appears to be a promising approach.

In this paper, we describe the generation of the first conditional Fatp4-deficient mouse line at all. This mouse line displays distinct changes in the structure of the epidermis and a compromised epidermal barrier function resembling the changes in mice with generalized Fatp4 deficiency. Thus, we show that the function of Fatp4 in keratinocytes is essential for the maintenance of a normal epidermal structure.

Certain features of newborn mice with generalized Fatp4 deficiency could not be observed in our mice with epidermis-specific Fatp4 deficiency, like the flat dermal–epidermal junction, the reduced number of pilo-sebaceous structures, and the condensed dermis with compact collagen fibers. Whereas newborn mice with total Fatp4 deficiency can be recognized at first sight because of their characteristic appearance, *esi-Fatp4* mice are not distinguishable from their control littermates macroscopically. Possible explanations for the milder phenotype of adult *esi-Fatp4* mice in comparison with newborn mice with total Fatp4 deficiency are: (1) as described (Li *et al*, 2000), we treated mice at the age of 10 wk with tamoxifen for 5 consecutive days, and again for 5 consecutive days, 2, 4, and 6 wk later, and examined them 7 and 13 wk AFT, respectively. Possibly, this period of time might not be sufficient for the development of all alterations observed in newborn mice with generalized Fatp4 deficiency, and further changes in the skin architecture might become visible after a longer period of observation or a longer time course of tamoxifen treatment. (2) The recombination efficiency of K14-Cre-ER^{T2} might be below 100%. A small rest activity of Fatp4 in the epidermis of *esi-Fatp* mice might lead to a milder phenotype than in mice with total Fatp4 deficiency; however, we could not detect Fatp4 protein by immunofluorescence 7 or 13 wk AFT. Furthermore, Li *et al* (2000) already described a complete recombination of a floxed *RXR*α allele by K14-Cre-ER^{T2}. (3) Fatp4 might be more important for the generation than for the maintenance of the epidermal barrier.

The epidermis of mice with generalized *Fatp4* deficiency exhibits an abnormal lipid composition, the most striking difference being an increase of the ceramide fraction by about 80% and a decrease of very long chain fatty acids with at least 26 C atoms within the ceramide fraction from 64% to 26% in Fatp4-deficient mice (Herrmann *et al*, 2003). Although an analysis of the lipid composition of the epidermis of *esi-Fatp4* mice has not been performed, we assume that the mechanisms that lead to these very similar phenotypes are identical because of the identical underlying genetic cause. Of note, in addition to their structural role in the epidermis, ceramides are also involved in various signalling pathways that control differentiation and proliferation (Huwiler *et al*, 2000).

The availability of a mouse model with inducible epidermis-specific Fatp4 deficiency in the skin will enable further projects for analysis of the details of Fatp4 function in the skin of adult mice. By means of this mouse line, it will be possible to determine the sequence of morphological events that lead to the observed hyperkeratosis, to characterize the metabolic changes in Fatp4-deficient epidermis further, and to detect delayed consequences of the observed morphological and functional changes.

Materials and Methods

Genotyping of *Fatp4* alleles Genomic DNA was isolated from tissues by standard techniques. The epidermis was separated from the dermis after heating tail skin in distilled water to 64°C for 10 s. *Fatp4* genotyping was performed by PCR with primer pairs specific for the wt, the flox, the neoΔex3, and the Δex3 alleles, respectively.

Generation of *Fatp4* mutant mice The generation of *Fatp4* mutant mice has been reported previously (Herrmann *et al*, 2003). The original mouse line carried the mutant allele *Fatp4^{neoflox}* (*Fatp4-K*; Herrmann *et al*, 2003) harboring a gene trap cassette in intron 2 (Fig 1*A*). By crossing this mouse line with a transgenic mouse line expressing FLPe recombinase (Rodriguez *et al*, 2000), the gene trap cassette was excised, and the mutant allele *Fatp4^{neoflox}* was converted into the mutant allele *Fatp4^{flox}*, which carried two loxP sites within introns 2 and 3, respectively (Fig 1*A*). Mice homozygous for the "floxed" *Fatp4* allele showed no phenotypic abnormalities, indicating that the allele *Fatp4^{flox}* was functionally fully active. When mice carrying the *Fatp4^{flox}* allele were crossed with *PGK-Cre* transgenic mice (kindly provided by Klas Kullander and Ruediger Klein) exhibiting ubiquitous *Cre* expression (Schwenk *et al*, 1995), the *Fatp4^{flox}* allele was converted into the null allele *Fatp4$^{\Delta ex3}$* (Fig 1*A*). Offspring homozygous for the *Fatp4$^{\Delta ex3}$* or *Fatp4^{neoflox}* alleles were analyzed for morphological differences and were found to be identical (data not shown). All procedures were in compliance with the guidelines of the institutional animal care and use committees, and in accordance with governmental guidelines. Institutional approval was granted for all experiments.

To generate mice with tamoxifen-inducible *Fatp4* inactivation in the epidermis, mice carrying the *Fatp4^{flox}* allele were crossed with transgenic mice carrying the *K14-Cre-ER^{T2}* transgene that expresses the tamoxifen-inducible Cre-ER^{T2} recombinase specifically in keratinocytes (Li *et al*, 2000). The resulting mice used for the experiments had a mixed genetic background C57BL/6–129SV/Ola.

Tamoxifen treatment As described (Li *et al*, 2000), tamoxifen (Sigma, St. Louis, Missouri; 0.1 mg in 100 μL sunflower oil) was injected intraperitoneally into female mice at the age of 10 wk for 5 consecutive days, and again for 5 consecutive days, 2, 4, and 6 wk later. Animals were sacrificed 7 or 13 wk AFT, and tissues were analyzed by histology, immunohistochemistry, and electron microscopy.

Histological analysis Histological analysis of the heart, lung, liver, spleen, kidney, stomach, duodenum, jejunum, ileum, colon, skeletal muscle, adipose tissue, and skin from dorsal and ventral trunk, ears, eyelids, snout, feet, and tail from control and tamoxifen-treated (7 wk AFT and 13 wk AFT) mice was performed as described previously (Herrmann *et al*, 2003).

Antibodies The primary antibodies used in immunohistochemistry were as follows: (1) guinea-pig antibodies against mouse Fatp4 (1:500; Herrmann *et al*, 2003), K14 (1:3000), K2e (1:2000) (both from Progen Biotechnik, Heidelberg, Germany), (2) mouse antibodies against transglutaminase 1 (1:20, CellSystems, St. Katharinen, Germany), (3) rabbit antibodies against keratin K10 (1:500, Covance, Denver, Pennsylvania), filaggrin (1:500, Covance), claudin-1 (1:100, Neomarkers Labvision, Fremont, California), loricrin (1:500, Covance), periplakin (1:500, a gift from Dr D. Hohl, Baylor College, Houston, Texas), and keratin K6 (1:500, Covance), (4) rat antibodies against Ki-67 (1:200, clone TEC-3, DAKO, Glostrup, Denmark).

The secondary antibodies used for indirect immunofluorescence were goat antibodies to guinea-pig, rabbit, mouse, or rat

immunoglobulins, coupled to Alexa 568 (dilution of 1:200; Molecular Probes, Eugene, Oregon).

Immunofluorescence microscopy and electron microscopy Indirect immunofluorescence microscopy procedures for membrane-associated proteins and cytoskeletal components were essentially performed as described in Herrmann *et al* (2003) (see also Schmidt *et al*, 1997; Langbein *et al*, 2002a). All investigations were performed in parallel on foot sole and snout skin of mice 7 and 13 wk AFT. In brief, the standard protocol was applied by using cryostat sections of freshly frozen tissues, fixed in acetone (5 min at -20°C), permeabilized with 0.1% Triton X-100/PBS for 2 min, followed by blocking with 5% normal goat serum in PBS. Primary and secondary antibodies were applied for ca. 45 min. For Fatp4 protein demonstration, various fixative protocols were used to prevent loss of soluble proteins (see protocols 2 and 3; Schmidt *et al*, 1997). The tissues were fixed with formaldehyde and antibodies applied for 45 min, or for a shorter time without using any detergents. Negative control immunostaining reactions were performed using non-immunized serum instead of the primary antibodies at the respective dilution or only the secondary antibody against immunoglobulins of the respective species. All of them were found to be negative. Moreover, "internal controls" exist by using the panel of different antibodies of several species indicated in the paragraph "Antibodies." DAPI for nuclear counterstaining was added to the secondary antibodies. Visualization and documentation were done by using a photomicroscope (Axiophot II, Carl Zeiss, Germany).

Electron microscopical investigations on the skin of *esi-Fapt4* and control mice 7 and 13 wk AFT were conducted as described in Herrmann *et al* (2003).

Skin permeability assays The diffusion of 1 mM Lucifer yellow in Ringer's solution (pH 7.4) at 37°C was analyzed as described (Matsuki *et al*, 1998). The frozen ear skin samples of animals 7 and 13 wk AFT, respectively, were sliced at a thickness of 5 μm and the sections were analyzed by fluorescence microscopy.

In addition, barrier-dependent access of X-gal to untreated skin was examined as described (Hardman *et al*, 1998).

We thank A. Peter, P. Hornsberger, G. Schmidt, S. Kaden, and S. Praetzel for their expert technical assistance. This work was supported by grants from the Deutsche Forschungsgemeinschaft (STR 216/11-1) and the Dietmar-Hopp-Foundation to W. Stremmel, and the Faculty of Medicine, University of Heidelberg to T. Herrmann.

DOI: 10.1111/j.0022-202X.2005.23972.x

Manuscript received April 26, 2005; revised July 9, 2005; accepted for publication August 6, 2005

Address correspondence to: Wolfgang Stremmel, Department of Internal Medicine IV, University of Heidelberg, Im Neuenheimer Feld 410, 69120 Heidelberg, Germany. Email: wolfgang.stremmel@email.de, thomas_herrmann@med.uni-heidelberg.de

References

Brandner JM, Kief S, Grund C, *et al*: Organization and formation of the tight junction system in human epidermis and cultured keratinocytes. Eur J Cell Biol 81:253–263, 2002

Brocard J, Feil R, Chambon P, Metzger D: A chimeric Cre recombinase inducible by synthetic, but not by natural ligands of the glucocorticoid receptor. Nucleic Acids Res 26:4086–4090, 1998

Coulombe PA, Kopan R, Fuchs E: Expression of keratin K14 in the epidermis and hair follicle: Insights into complex programs of differentiation. J Cell Biol 109:2295–2312, 1989

Dean JCS, Gray ES, Stewart KN, Brown T, Lloyd DJ, Smith NC, Pope FM: Restrictive dermopathy: A disorder of skin differentiation with abnormal integrin expression. Clin Genet 44:287–291, 1993

Feil R, Wagner J, Metzger D, Chambon P: Regulation of Cre recombinase activity by mutated estrogen receptor ligand-binding domains. Biochem Biophys Res Commun 237:752–757, 1997

Gimeno RE, Hirsch DJ, Punreddy S, *et al*: Targeted deletion of fatty acid transport protein-4 results in early embryonic lethality. J Biol Chem 278:49512–49516, 2003

Hall AM, Wiczer BM, Herrmann T, Stremmel W, Bernlohr DA: Enzymatic properties of purified murine fatty acid transport protein 4 and analysis of acyl-CoA synthetase activities in tissues from FATP4 null mice. J Biol Chem 280:11948–11954, 2005

Hardman MJ, Paraskevi S, Banbury DN, Byrne C: Patterned acquisition of skin barrier function during development. Development 125:1541–1552, 1998

Herrmann T, Buchkremer F, Gosch I, Hall AM, Bernlohr DA, Stremmel W: Mouse fatty acid transport protein 4 (FATP4): Characterization of the gene and functional assessment as a very long chain acyl-CoA synthetase. Gene 270:31–40, 2001

Herrmann T, van der Hoeven F, Gröne H-J, *et al*: Mice with targeted disruption of the fatty acid transport protein 4 (Fatp 4, Slc27a4) gene show features of lethal restrictive dermopathy. J Cell Biol 161:1105–1115, 2003

Holbrook KA, Dale BA, Witt DR, Hayden MR, Toriello HV: Arrested epidermal morphogenesis in three newborn infants with a fatal genetic disorder (restrictive dermopathy). J Invest Dermatol 88:330–339, 1987

Hughes BR, Morris C, Cunliffe WJ, Leigh IM: Keratin expression in pilosebaceous epithelia in truncal skin of acne patients. Br J Dermatol 134:247–256, 1996

Huwiler A, Kolter T, Pfeilschifter J, Sandhoff K: Physiology and pathophysiology of sphingolipid metabolism and signaling. Biochim Biophys Acta 1485:63–99, 2000

Langbein L, Grund C, Kuhn C, *et al*: Tight junctions and compositionally related junctional structures in mammalian stratified epithelia and cell cultures derived therefrom. Eur J Cell Biol 81:419–435, 2002a

Langbein L, Rogers MA, Praetzel S, Aoki N, Winter H, Schweizer J: A novel epithelial keratin, hK6irs1, is expressed differentially in all layers of the inner root sheath, including specialized Huxley cells (*"Flügelzellen"*) of the human hair follicle. J Invest Dermatol 118:789–800, 2002b

Langbein L, Rogers MA, Praetzel S, Winter H, Schweizer J: K6irs1, K6irs 2, K6irs 3, and K6irs 4 represent the inner-root-sheath (IRS)-specific type II epithelial keratins of the human hair follicle. J Invest Dermatol 120:512–522, 2003

Langbein L, Rogers MA, Winter H, Praetzel S, Beckhaus U, Rackwitz HR, Schweizer J: The catalog of human hair keratins: I. Expression of the nine type I members in the hair follicle. J Biol Chem 274:19874–19893, 1999

Langbein L, Rogers MA, Winter H, Praetzel S, Schweizer J: The catalog of human hair keratins: II. Expression of the six type II members in the hair follicle and the combined catalog of human type I and type II keratins. J Biol Chem 276:35123–35132, 2001

Langbein L, Schweizer J: The keratins of the human hair follicle. Int Rev Cytol 243:1–78, 2005

Li M, Indra AK, Warot X, *et al*: Skin abnormalities generated by temporally controlled RXR-alpha mutations in mouse epidermis. Nature 407:633–636, 2000

Logie C, Stewart AF: Ligand-regulated site-specific recombination. Proc Natl Acad Sci USA 92:5940–5944, 1995

Matsuki M, Yamashita F, Ishida-Yamamoto A, *et al*: Defective stratum corneum and early neonatal death in mice lacking the gene for transglutaminase 1 (keratinocyte transglutaminase). Proc Natl Acad Sci USA 95:1044–1049, 1998

Metzger D, Chambon P: Site- and time-specific gene targeting in the mouse. Methods 24:71–80, 2001

Metzger D, Clifford J, Chiba H, Chambon P: Conditional site-specific recombination in mammalian cells using a ligand-dependent chimeric Cre recombinase. Proc Natl Acad Sci USA 92:6991–6995, 1995

Morita K, Furuse M, Fujimoto K, Tsukita S: Claudin multigene family encoding four-transmembrane domain protein components of tight junction strands. Proc Natl Acad Sci USA 96:511–516, 1999

Moulson CL, Martin DR, Lugus JJ, Schaffer JE, Lind AC, Miner JH: Cloning of wrinkle-free, a previously uncharacterized mouse mutation, reveals crucial roles for fatty acid transport protein 4 in skin and hair development. Proc Natl Acad Sci USA 100:5274–5279, 2003

Rodriguez CI, Buchholz F, Galloway J, *et al*: High-efficiency deleted mice show that FLPe is an alternative to Cre-loxP. Nat Genet 25:139–140, 2000

Schmidt A, Langbein L, Rode M, Praetzel S, Zimbelmann R, Franke WW: Plakophilins 1a and 1b: Widespread nuclear proteins recruited in specific epithelial cells as desmosomal plaque components. Cell Tiss Res 29:481–499, 1997

Schwenk F, Baron U, Rajewsky K: A cre-transgenic mouse strain for the ubiquitous deletion of loxP-flanked gene segments including deletion in germ cells. Nucleic Acids Res 23:5080–5081, 1995